


Quantum Tunneling of Protons through Respiratory Complex I of Mitochondria

Abdallah Barjas Qaswal ^{1,*}, Hala Raed Miqdadi ¹, Heba Lala ², Renad Alawamleh ², Areen Altarawneh ², Sanaa Kasho ², Mujahed Maghnem ², Refa Almiani ², Manar Abu Awwad ², Zaid Albzour ², Yasmeen Alnsour ³, Dana Elmughrabi ⁴, Rawan Abudawood ⁴, Duaa Dahbour ⁵, Rasha Alatout ⁶, Nedal Alemleh ⁶, Abdallah Hamdan ⁶, Maryam Alsamaraie ⁶, Abdallah Awni Ismail ², Ahmad Al-Momani ², Amro Almomani ⁷, Motaz Barakat ⁸, Jihad Feras AlSamhori ⁷

¹ Department of Psychiatry, Jordan University Hospital, Amman 11942, Jordan; qaswalabdullah@gmail.com (A.B.Q.); halamiqdadi@gmail.com (H.R.M.);

² Department of Internal Medicine, University of Jordan, Amman 11942, Jordan; hbh8201462@ju.edu.jo (H.L.); alawamleh_renad@yahoo.com (R.A.); Areentarawneh6@gmail.com (A.A.); Sanaaqasho@yahoo.com (S.K.); Mujahedmaghnam@gmail.com (M.M.); rafaa_maani@yahoo.com (R.A.); manarabuawwad6@gmail.com (M.A.A.); zaid.bzour@yahoo.com (Z.A.); Abdallahboreny1997@gmail.com (A.A.I.); Ahmad.al.momani@hotmail.com (A.A.-M.);

³ Department of Anesthesia, School of Medicine, University of Jordan, Amman 11942, Jordan; yasmeensour96@outlook.com;

⁴ Department of Emergency and Accidents, Jordan University, Jordan, Amman 11942, Jordan; Danaalmughrabi@hotmail.com (D.E.); rawanabudawood96@gmail.com (R.A.);

⁵ Department of Gynecology and Obstetrics, University of Jordan, Amman 11942, Jordan; duaadahboor@outlook.com;

⁶ Department of General Surgery, University of Jordan, Amman 11942, Jordan; Rasha27alatout61995@gmail.com (R.A.); nalamleh@yahoo.com (N.A.); dr-a.hamdan@outlook.com (A.H.); maryamkanan12@gmail.com (M.A.);

⁷ School of Medicine, The University of Jordan, Amman 11942, Jordan; amromomani123@gmail.com (A.A.); jehadsam2000@gmail.com (J.F.A.);

⁸ Department of Maxillofacial Surgery, Jordan University Hospital, Amman 11942, Jordan; motzbarakat1@gmail.com;

* Correspondence: qaswalabdullah@gmail.com;

Received: 10.03.2025; Accepted: 21.05.2025; Published: 9.08.2025

Abstract: Mitochondria are the major cellular organelles responsible for ATP production. They produce ATP through the process of oxidative phosphorylation, in which the proton motive force (pmf) is the driving force by which protons pass through ATPase. The pmf is generated by the pumping activity of the electron transport chain ETC, particularly complexes I, III, and IV. As the proton can be physically described as a quantum wave, it is important to explore the role of the quantum behavior in its transport through the ETC proteins, particularly the respiratory complex I. In the present study, the potential functions of three subunits of complex I were identified, and the Schrödinger equation was solved numerically by the finite difference method using MATLAB to obtain the eigenstates and their corresponding eigenvalues. In addition, quantum tunneling probability and quantum conductance values were calculated using WKB approximation for the eigenenergies of the proton in each potential barrier. Moreover, entropic tunneling delay time and tunneling currents were calculated. Our results indicate that quantum tunneling transport yields significant values of quantum conductance that can contribute significantly to the pmf while utilizing less than 45 % of the required energy to overcome the barriers of the subunits in respiratory complex I.

Keywords: quantum tunneling; mitochondria; respiratory complex I; quantum biology; membrane potential; proton.

© 2025 by the authors. This article is an open-access article distributed under the terms and conditions of the Creative Commons Attribution (CC BY) license (<https://creativecommons.org/licenses/by/4.0/>), which permits unrestricted use, distribution, and reproduction in any medium, provided the original work is properly cited. The authors retain copyright of their work, and no permission is required from the authors or the publisher to reuse or distribute this article, as long as proper attribution is given to the original source.

1. Introduction

Mitochondria are the major cellular organelles that produce energy in the form of adenosine triphosphate (ATP) [1,2]. The production of ATP molecules is achieved by generating a driving force of protons from the intermembrane space (IMS) to the matrix of the mitochondria to pass through a crucial protein called ATPase enzyme that converts adenosine diphosphate (ADP) to ATP [1,2]. Hence, the energy of proton flow is utilized by ATPase to produce the ATP [1,2]. The proton flow from IMS to the matrix is driven by the electrochemical gradient of protons, which means that the concentration of protons in IMS is higher than in the matrix, and the membrane potential of the inner mitochondrial membrane (IMM) is negative at the matrix side relative to the IMS side [1,2]. This electrochemical gradient is sustained by the electron transport chain (ETC), which pumps protons against their concentration gradient to the IMS side [3]. The ETC is composed of several proteins through which electrons pass and mediate redox reactions, and thus, energy is released to pump protons against their concentration gradient. These proteins include complex I, complex II, coenzyme Q, complex III, cytochrome c, and complex IV. Complexes I, III, and IV are the only ETC proteins that utilize the energy released from redox reactions to pump protons and contribute to the electrochemical gradient [4]. Respiratory complex 1 has recently gained attention to explore the molecular dynamics of proton flow [5–7]. Previous studies showed that it is composed of several subunits that act as antiporters for protons, especially ND2, ND4, and ND5 subunits [5–7]. They form horizontal and lateral pathways for proton transfer mediated by protonation/deprotonation of amino acid residues of respiratory complex 1, resulting in water-wired conduction routes. These pathways form energetic barriers for the proton passage, which are modulated by ion pairs [5]. The closed ion pairs increase the heights of the barrier, while the open ones lower them. Recently, the free energy profiles of protons have been determined, revealing the shapes of the barriers in ND2, ND4, and ND5 subunits [5]. There are two major types of transport of protons through such barriers, which are classical transport and quantum tunneling transport. Classical transport implies that protons can pass through a barrier only when their energy overcomes the height of the barrier, while quantum tunneling transport refers to the possibility of the passage of protons when their energy is lower than the potential energy of the barrier.

Investigating the quantum phenomena within biological systems falls within the scope of quantum biology [8,9]. Quantum biology is the scientific field that explores biological processes and functions using the principles of quantum mechanics. Protons have received considerable attention in the context of quantum biology as researchers investigated the role of proton tunneling in the catalytic activity of enzymes and DNA point mutations [10,11]. In addition, the mitochondrion is an interesting molecular target that may exploit the quantum behavior of protons and electrons for optimal functioning [12–14]. In the present work, we aim to study the possible contribution of the quantum behavior of protons in the process of ATP production. Specifically, the current work aims to investigate the quantum tunneling transport of protons through the respiratory complex I and its contribution to the proton motive force (pmf).

2. Materials and Methods

The respiratory complex I is a major component of ETC that pumps protons against their concentration gradient from the matrix to the IMS, exploiting the energy released from the transfer of electrons. See Figure 1. Based on the energetics of the antiporter-like subunits of the respiratory complex I, three subunits were studied, and their energy profiles were obtained [5]. Each of these subunits contains a horizontal pathway with a potential barrier made by the protonated/deprotonated amino acids [5]. Using cubic spline fitting, we can represent the profiles mathematically by potential functions $V(x)$ using MATLAB software. We use this fitting to capture the complexity of the potential functions.

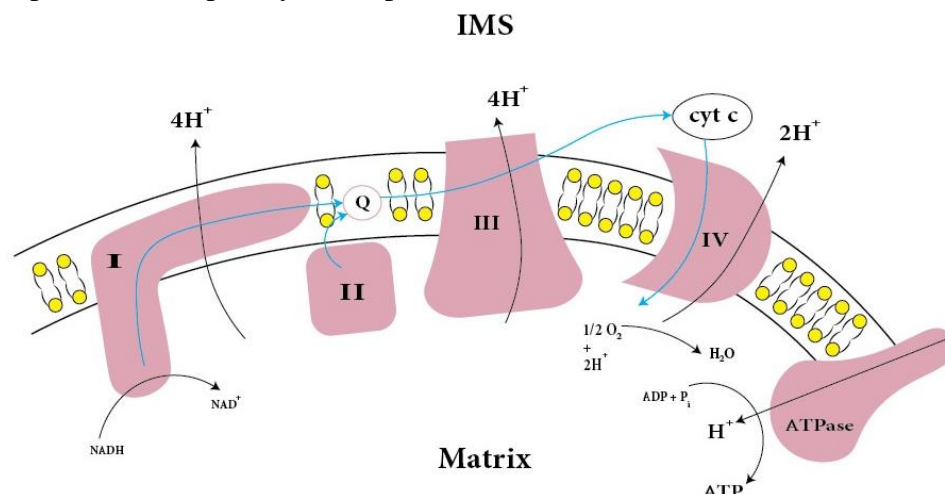


Figure 1. The figure represents a schematic diagram of the electron transport chain ETC and the transport of electrons (represented by the blue arrows) and protons.

The potential function of the subunit ND2 can be written as follows:

$$V_1(x) = \begin{cases} A(-0.9582(ax+5)^3 + 3.8869(ax+5)^2 - 0.9287(ax+5)), & -5 \times 10^{-10} \leq x < -4 \times 10^{-10} \\ A(-0.9582(ax+4)^3 + 1.0124(ax+4)^2 + 3.9706(ax+4) + 2), & -4 \times 10^{-10} \leq x < -2.5 \times 10^{-10} \\ A(0.4653(ax+2.5)^3 - 3.2993(ax+2.5)^2 + 0.5402(ax+2.5) + 7), & -2.5 \times 10^{-10} \leq x < 0 \\ A(2.0419x^3 + 0.1903x^2 - 7.2322x - 5), & 0 \leq x < 1 \times 10^{-10} \\ A(-2.59(ax-1)^3 + 6.3159(ax-1)^2 - 0.7259(ax-1) - 10), & 1 \times 10^{-10} \leq x < 2 \times 10^{-10} \\ A(-0.6820(ax-2)^3 - 1.4540(ax-2)^2 + 4.1360(ax-2) - 7), & 2 \times 10^{-10} \leq x < 3 \times 10^{-10} \\ A(-0.6820(ax-3)^3 - 3.5(ax-3)^2 - 0.8180(ax-3) - 5), & 3 \times 10^{-10} \leq x \leq 4 \times 10^{-10} \end{cases} \quad (1)$$

The potential function of the subunit ND4 can be written as follows:

$$V_2(x) = \begin{cases} A(-2.68(ax+5)^3 + 8.55(ax+5)^2 - 2.87(ax+5)), & -5 \times 10^{-10} \leq x < -4 \times 10^{-10} \\ A(-2.68(ax+4)^3 + 0.5(ax+4)^2 + 6.18(ax+4) + 3), & -4 \times 10^{-10} \leq x < -3 \times 10^{-10} \\ A(3.64(ax+3)^3 - 7.55(ax+3)^2 - 0.87(ax+3) + 7), & -3 \times 10^{-10} \leq x < -1.5 \times 10^{-10} \\ A(-3.69(ax+1.5)^3 + 8.83(ax+1.5)^2 + 1.06(ax+1.5) + 1), & -1.5 \times 10^{-10} \leq x < 0 \\ A(2.13(ax)^3 - 7.77(ax)^2 + 2.64(ax) + 10), & 0 \leq x < 1 \times 10^{-10} \\ A(2.91(ax-1)^3 - 1.39(ax-1)^2 - 6.52(ax-1) + 7), & 1 \times 10^{-10} \leq x < 2 \times 10^{-10} \\ A(-3.78(ax-2)^3 + 7.35(ax-2)^2 - 0.57(ax-2) + 2), & 2 \times 10^{-10} \leq x < 3 \times 10^{-10} \\ A(-3.78(ax-3)^3 - 4(ax-3)^2 + 2.78(ax-3) + 5), & 3 \times 10^{-10} \leq x \leq 4 \times 10^{-10} \end{cases} \quad (2)$$

And the potential function of the subunit ND5 can be written as follows:

$$V_3(x) = \begin{cases} A(-2.7113(ax+3)^3 + 9.1339(ax+3)^2 - 4.4226(ax+3)), & -3 \times 10^{-10} \leq x < -2 \times 10^{-10} \\ A(-2.7113(ax+2)^3 + (ax+2)^2 + 5.7113(ax+2) + 2), & -2 \times 10^{-10} \leq x < -1 \times 10^{-10} \\ A(4.5565(ax+1)^3 - 7.1339(ax+1)^2 - 0.4226(ax+1) + 6), & -1 \times 10^{-10} \leq x < 0 \\ A(-4.5149(ax)^3 + 6.5357(ax)^2 - 1.0208(ax) + 3), & 0 \leq x < 1 \times 10^{-10} \\ A(2.5030(ax-1)^3 - 7.0089(ax-1)^2 - 1.4940(ax-1) + 4), & 1 \times 10^{-10} \leq x < 2 \times 10^{-10} \\ A(2.5030(ax-2)^3 + 0.5000(ax-2)^2 - 8.0030(ax-2) - 2), & 2 \times 10^{-10} \leq x \leq 3 \times 10^{-10} \end{cases} \quad (3)$$

Where A is the scaling factor of 7×10^{-21} J/Kcal mol⁻¹ to convert the unit of the potential energy from Kcal mol⁻¹ to J and a is the scaling factor of 1×10^{10} .

Accordingly, the potential functions of the three barriers can be plotted to help visualize their shapes and to explore their characteristics, as shown in Figure 2.

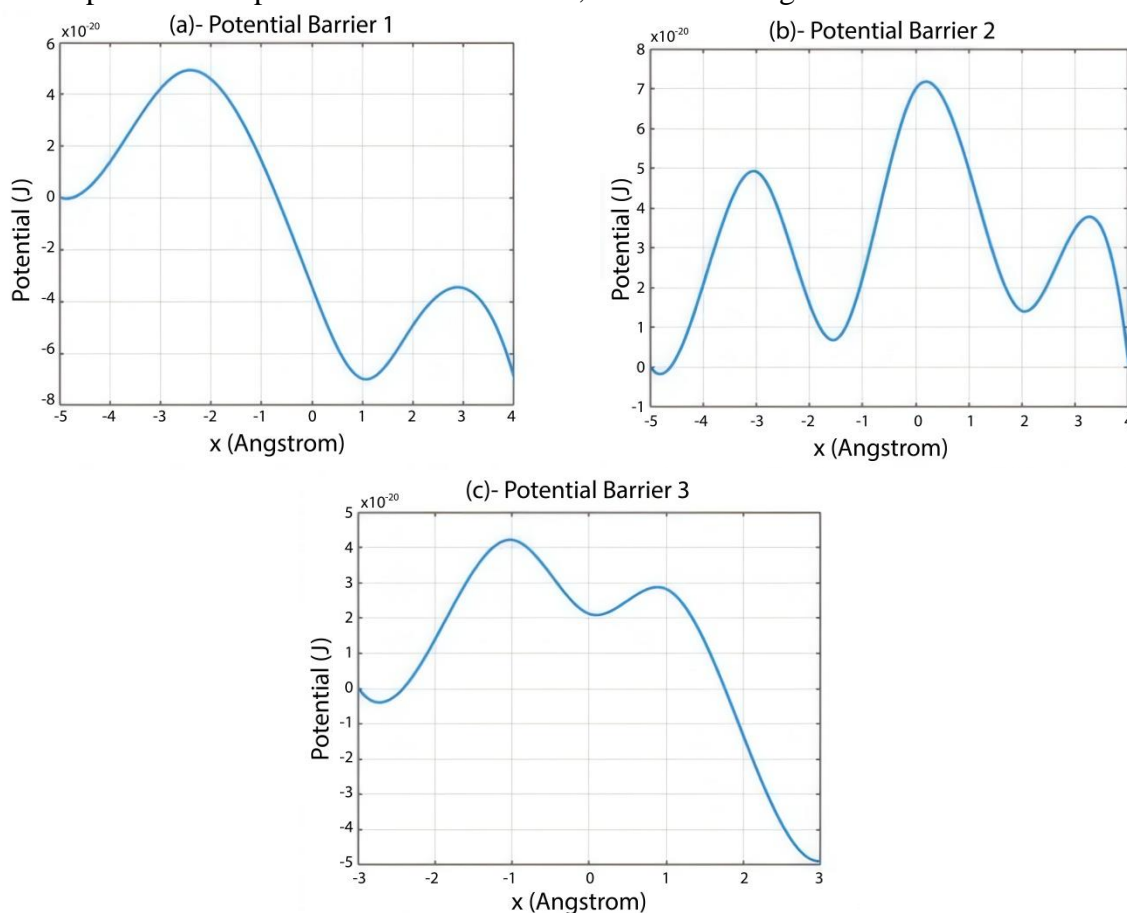


Figure 2. The figure represents the potential functions for three barriers in the respiratory complex I of mitochondria. **(a)** the potential barrier 1, which represents the energetic barrier of subunit ND2; **(b)** the potential barrier 2, which represents the energetic barrier of subunit ND4; **(c)** the potential barrier 3, which represents the energetic barrier of subunit ND5.

By comparing the plots in Figure 2 with the energy profiles obtained using density functional theory (DFT) and the hybrid QM/MM simulation in this study [5], these plots capture the essential features of the energy profiles, including the shape of the barrier, the range and the scale of the proton position within the pathway, and the range and the scale of the potential energy of the proton. The only difference is that we use the SI unit of energy Joule (J), instead of Kcal/mol.

To elucidate the multiple heights in each barrier, see Figure 3. Each height represents the minimum energy required for a proton to pass over classically. In addition, each height is

calculated as the absolute difference between the minimum and the maximum from left to right of the plot. See Figure 3.

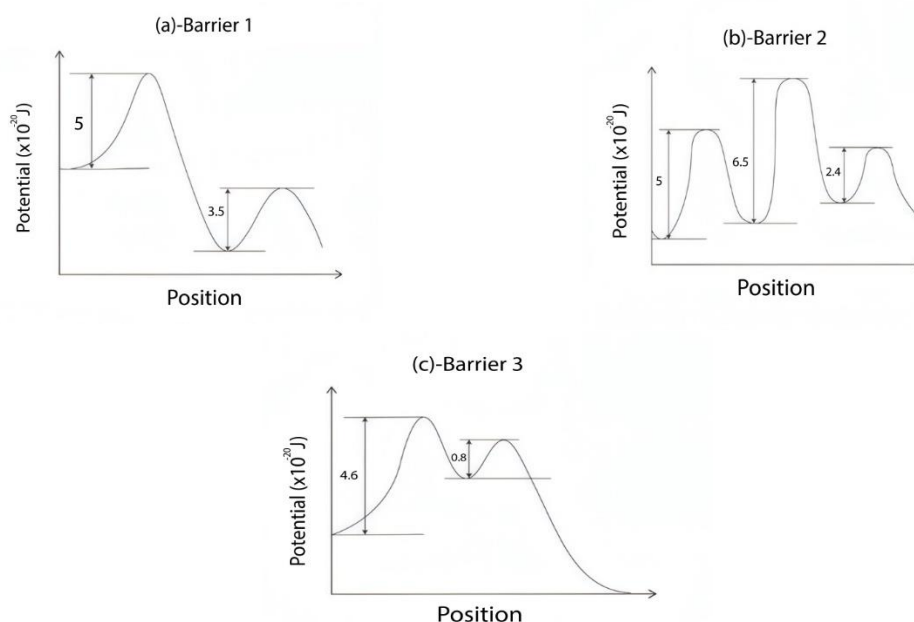


Figure 3. The figure represents a schematic diagram of the barrier heights in each subunit of the respiratory complex I.

The quantum tunneling probability of a proton through the potential barrier can be calculated using 1-D Wentzel–Kramers–Brillouin (WKB) method by the following equation [15,16]:

$$T_Q = \exp\left(-\frac{2\sqrt{2m}}{\hbar} \int_{x_1}^{x_2} \sqrt{V(x) - E} dx\right) \quad (4)$$

Where T_Q is the quantum tunneling probability, m is the mass of the proton, \hbar is the reduced Planck constant, $V(x)$ is the potential function, E is the energy of the proton, and x_1 and x_2 are where $V(x)=E$.

Accordingly, protons can behave as waves that can tunnel through the potential barrier of the three subunits of complex I. See Figure 4.

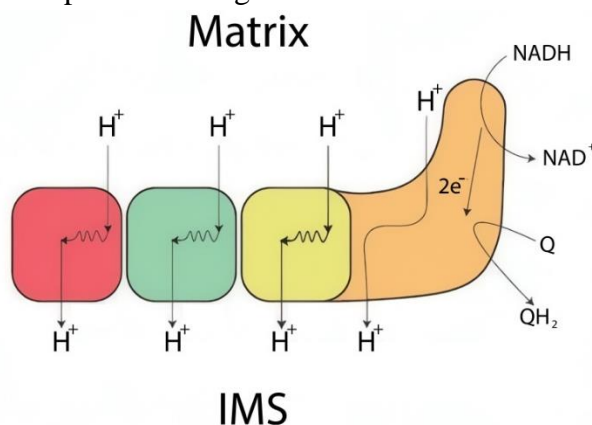


Figure 4. A schematic diagram represents the quantum tunneling of protons through the horizontal pathways of the three subunits of complex I, which are ND2, ND4, and ND5. Quantum tunneling is represented by the wavy arrow.

Eventually, the quantum unitary conductance C_Q and the quantum membrane conductance MC_Q of respiratory complex I can be calculated by the following equations, respectively [15–17]:

$$C_Q = \frac{q^2}{h} T_Q \quad (5)$$

$$MC_Q = C_Q D \quad (6)$$

Where q is the charge of the proton, h is the Planck constant, and D is the number of complex I proteins per surface area unit.

The quantum unitary conductance is the conductance of a single subunit of the three subunits of complex I, and the quantum membrane conductance is the sum of all conductance values that come from a certain number of subunits.

Recent studies focused on the proton tunneling delay time [18,19], which is the time required for the proton to pass the barrier via quantum tunneling. They identified two approaches to calculate it. These are the dwell time and the entropic time. The entropic tunneling delay time provided more consistent results, especially with the experimental observations [18,19]. Hence, the entropic tunneling delay time t_Q will be used in the present study. It can be calculated by the following equation [18,19]:

$$t_Q = -\frac{t_c}{P \log P} \quad (7)$$

Where $t_c = \int_{x1}^{x2} \frac{mdx}{\sqrt{2m(V(x)-E)}}$ and P is the probability of finding the proton in the barrier region, which can be calculated by the following equation [18,19]:

$$P = \int_{x1}^{x2} \psi(x) \psi^*(x) dx \quad (8)$$

Where $\psi(x)$ is the wave function and $\psi^*(x)$ is the complex conjugate of the wave function, which can be obtained by solving the Schrödinger equation.

The wave function can be obtained by solving the time-independent Schrödinger equation:

$$-\frac{\hbar^2}{2m} \frac{d^2 \psi(x)}{dx^2} + V(x) \psi(x) = E \psi(x) \quad (9)$$

In the case of having multiple heights in each barrier, as in Figure 3, equation (7) becomes:

$$t_Q = -\frac{\sum_{i=1}^n t_{c_i}}{\sum_{i=1}^n P_i \log \sum_{i=1}^n P_i} \quad (10)$$

Where n is the number of heights in each barrier.

The Schrödinger equation will be solved numerically using the finite difference method using MATLAB software.

In addition, the quantum tunneling current I_Q can be calculated using the following equation:

$$I_Q = \frac{q}{t_Q} T_Q \quad (11)$$

Eventually, the quantum tunneling of protons through respiratory complex I can affect the membrane potential of IMM at different energy levels according to the following equation [20]:

$$MC[H^+]_{IMS} = e^{\frac{-qV_m}{K_B T}} [H^+]_{Matrix} (MC + MC_Q) \quad (12)$$

Where MC is the classical membrane conductance of protons, $[H^+]_{IMS}$ is the concentration of protons in IMS, $[H^+]_{Matrix}$ is the concentration of protons in the matrix, MC_Q is the quantum membrane conductance of protons, V_m is the electrical potential of IMM, q is the charge of the proton, K_B is the Boltzmann constant, and T is the body temperature.

3. Results and Discussion

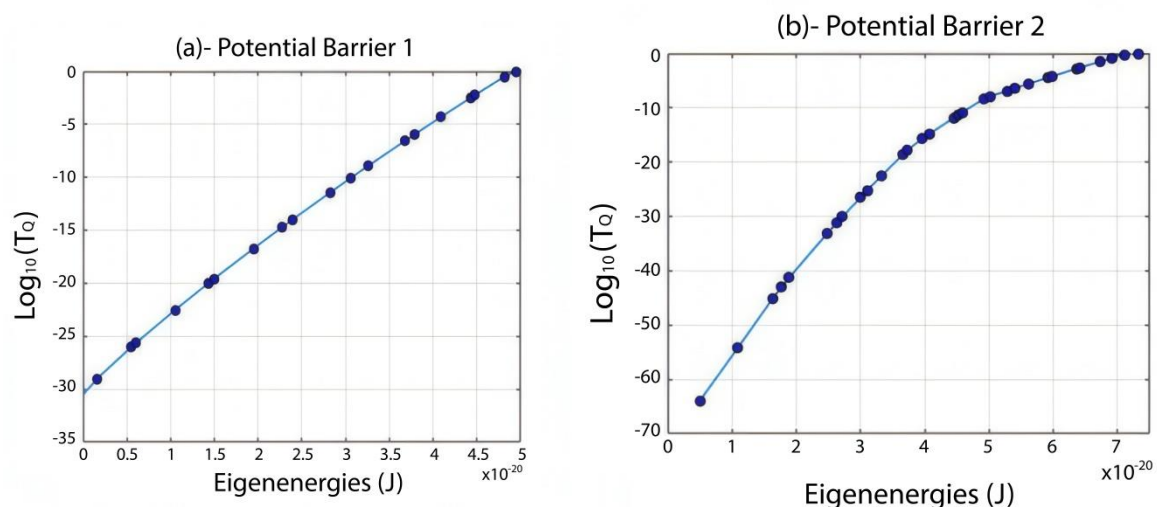
In this section, numerical results are calculated and plotted to help explore the relevance and the influence of the quantum tunneling of protons in generating the electrical potential of IMM. Table 1 shows the numerical values of the parameters related to mitochondria and their surrounding environment.

Table 1. The parameters related to mitochondria and their values.

Parameter	Value
The protons concentration in the matrix $[H^+]_{Matrix}$	1.58×10^{-5} mmol/L
The protons concentration in the IMS $[H^+]_{IMS}$	1×10^{-4} mmol/L
The charge of proton q	1.6×10^{-19} C
The Planck constant h	6.6×10^{-34} Js
The reduced Planck constant \hbar	1.05×10^{-34} Js
The Boltzmann constant K_B	1.38×10^{-23} J/K
The Body temperature T	310 K
The classical membrane conductance of protons MC	4 nS/cm ² [21]
Number of complex I proteins per surface area unit of IMM (D)	$10^{12} - 10^{14}$ m ⁻² [22–24]

3.1. The quantum tunneling probability of protons.

By solving the time-independent Schrödinger equation, eigenenergies can be obtained for the proton in each potential barrier. Then, the tunneling probability for each eigenenergy can be calculated using equation (4) after solving the integral for each barrier. See Figure 5.



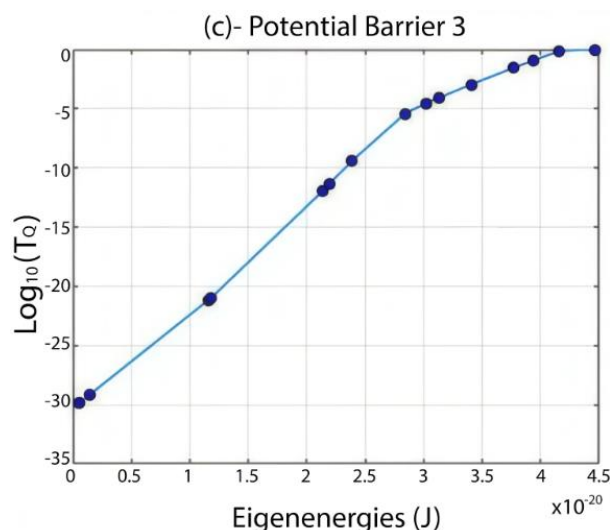


Figure 5. The figure represents the relationship between the common logarithm of tunneling probability and the eigenenergies for (a) barrier 1; (b) barrier 2; (c) barrier 3.

3.2. The quantum conductance of protons.

Based on equations (5) and (6), the quantum unitary conductance and the quantum membrane conductance can be calculated for each barrier. See Figure 6 and Figure 7.

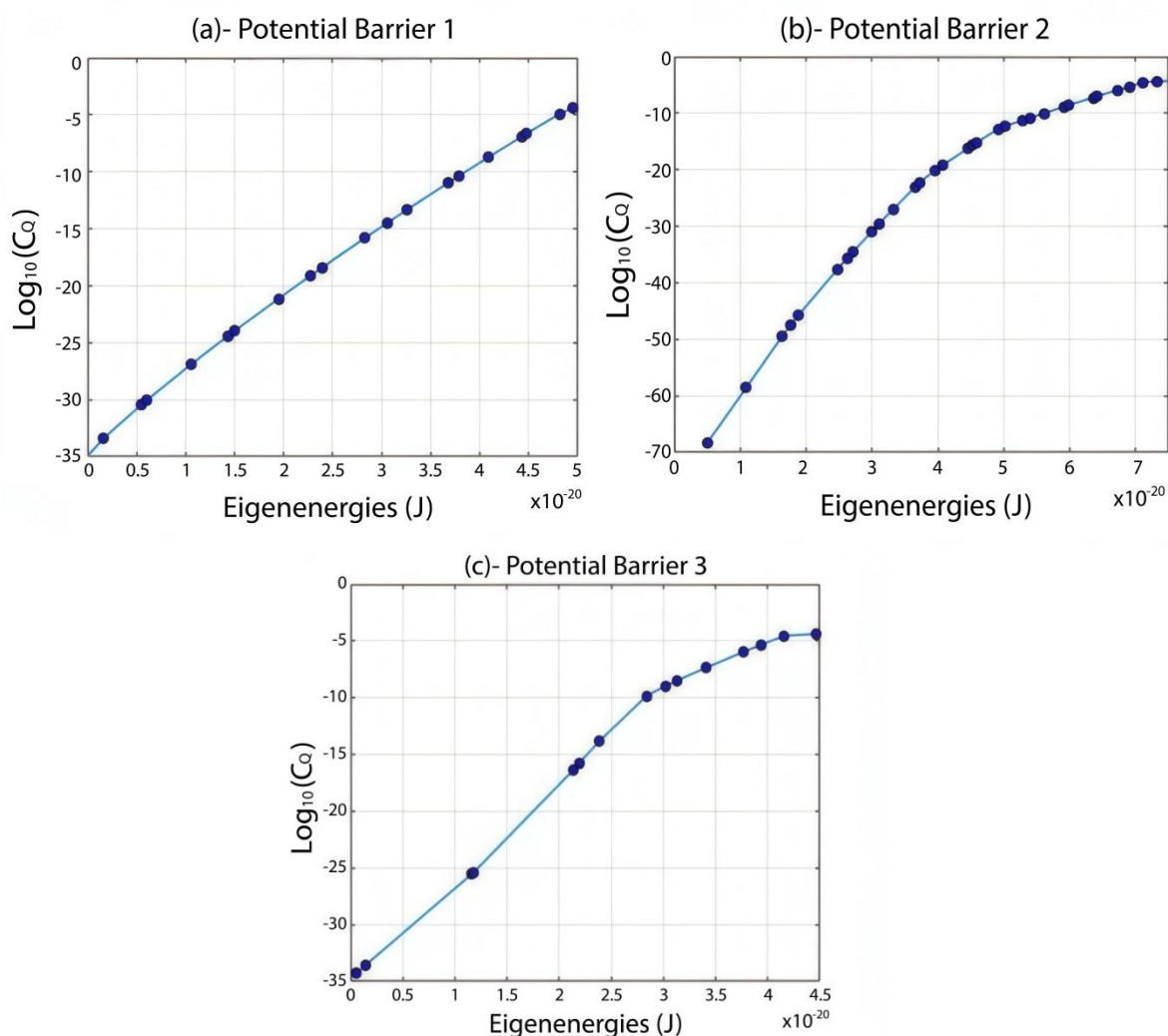


Figure 6. The figure represents the relationship between the common logarithm of quantum unitary conductance and the eigenenergies for (a) barrier 1; (b) barrier 2; (c) barrier 3.

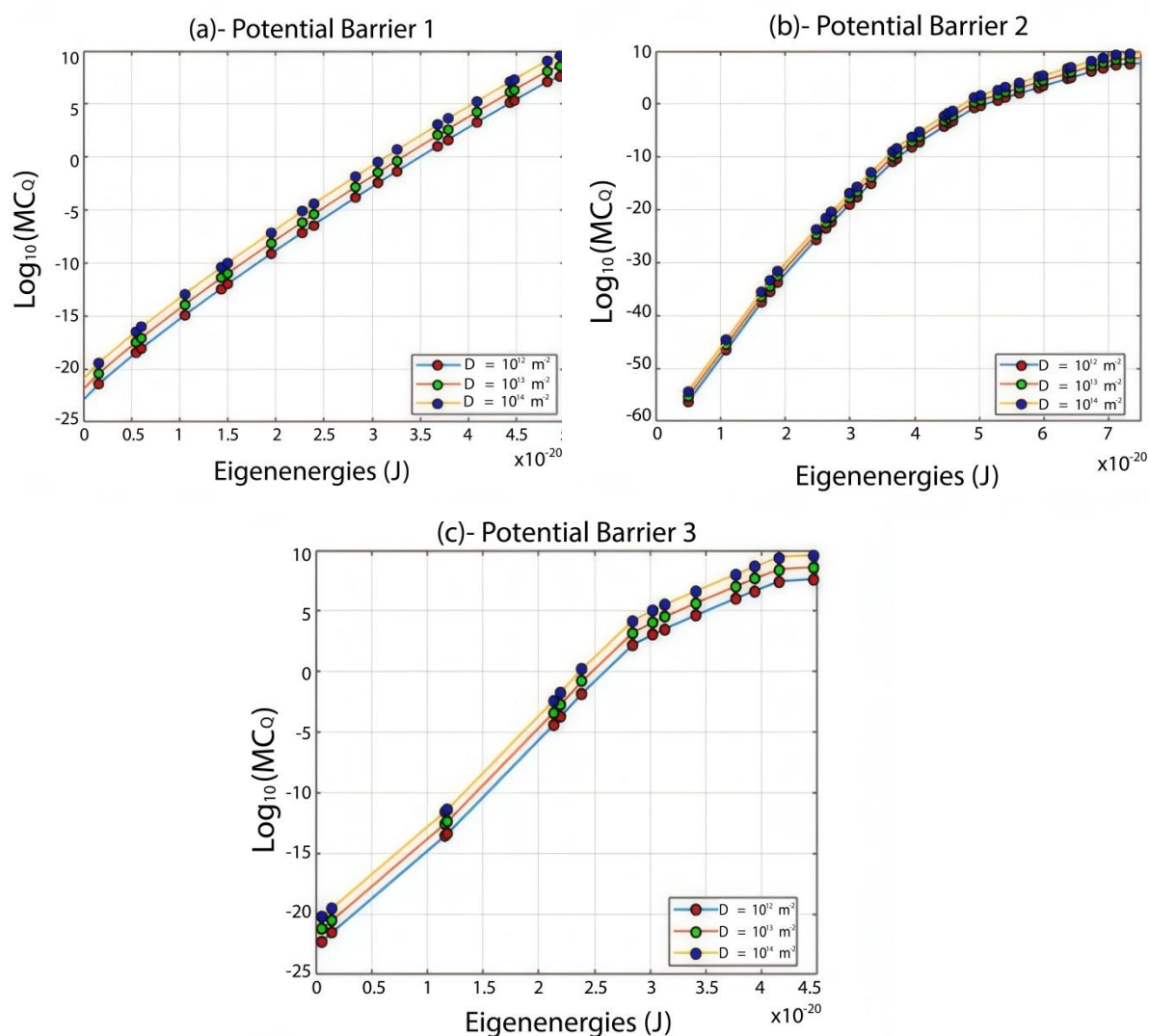
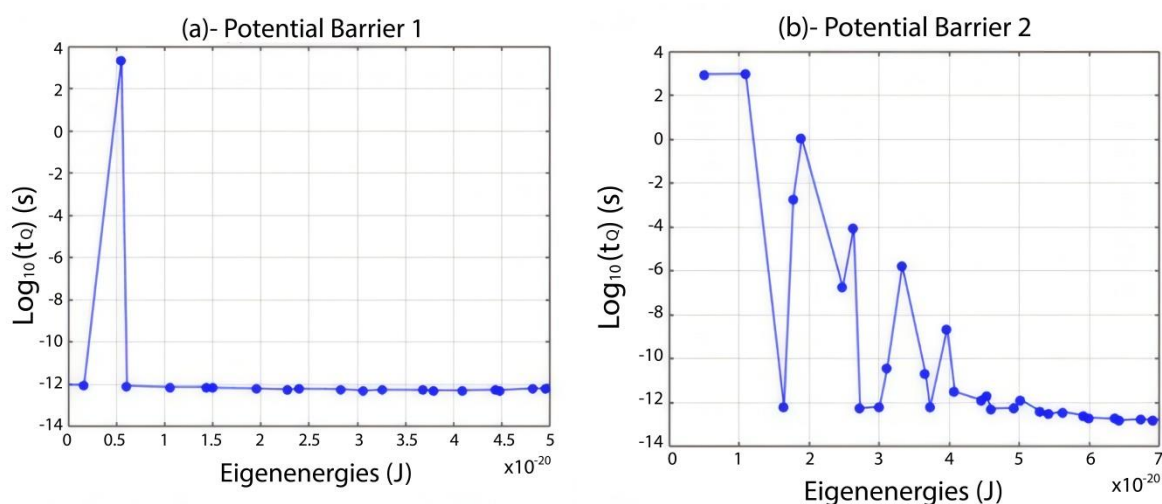


Figure 7. The figure represents the relationship between the common logarithm of the quantum membrane conductance and the eigenenergies for (a) barrier 1; (b) barrier 2 ; (c) barrier 3.

3.3. The quantum tunneling delay time.

Based on equations (7)-(10), the quantum tunneling delay time of the proton can be calculated. See Figure 8.



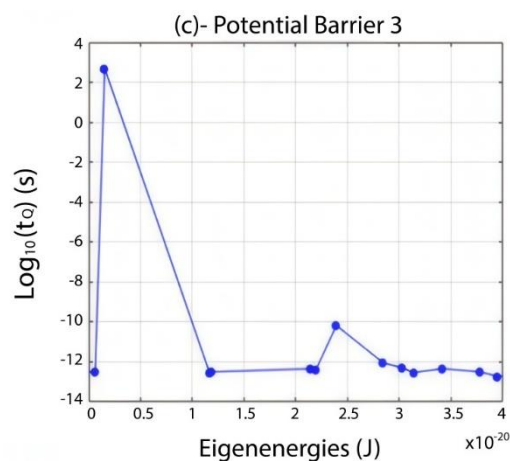


Figure 8. The figure represents the relationship between the common logarithm of tunneling delay time and the eigenenergies for (a) barrier 1; (b) barrier 2; (c) barrier 3.

3.4. The quantum tunneling currents.

Based on equation (11), the quantum tunneling currents of protons can be calculated for each barrier. See Figure 9.

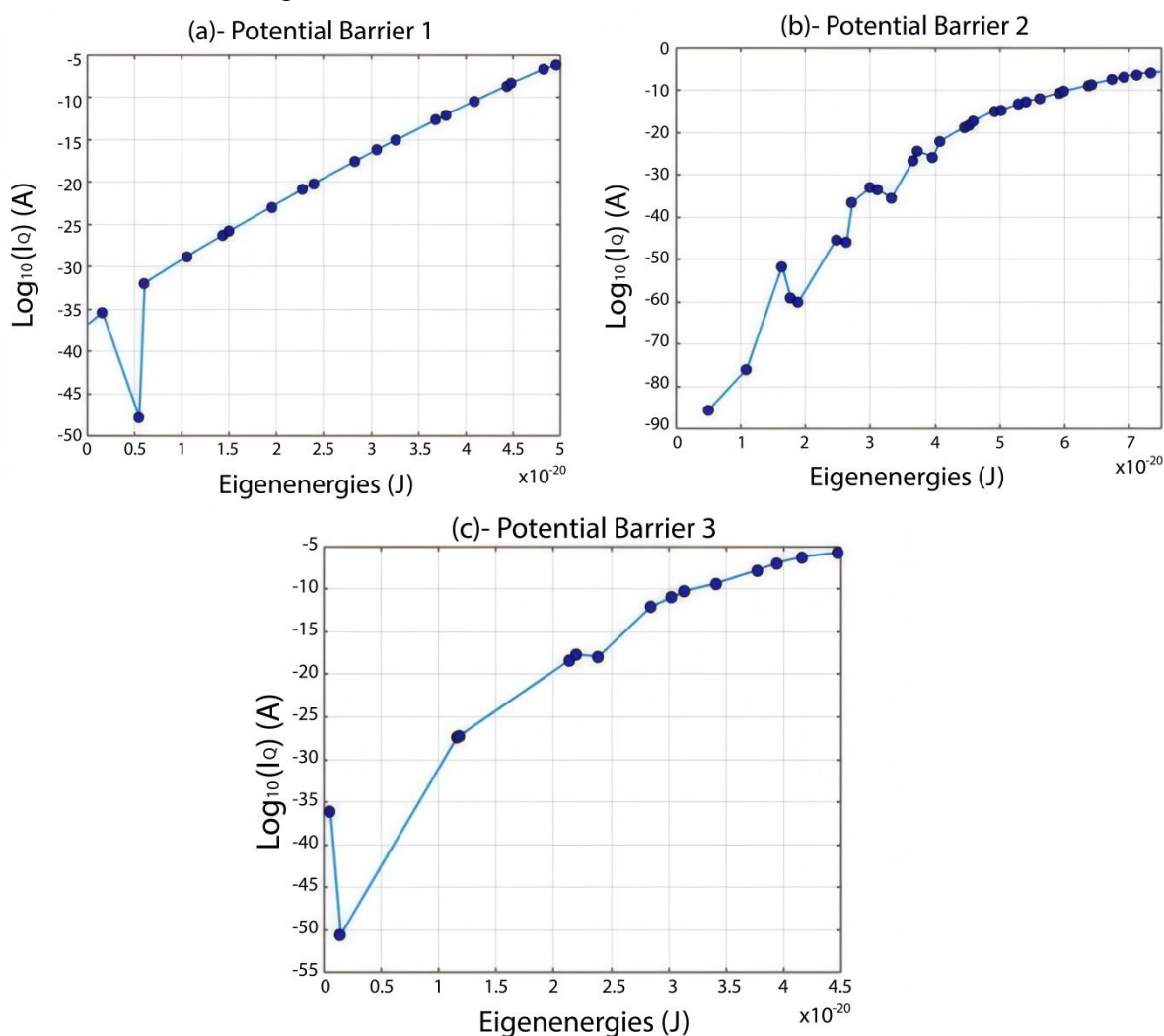


Figure 9. The figure represents the relationship between the common logarithm of quantum tunneling current and the eigenenergies for (a) barrier 1; (b) barrier 2; (c) barrier 3.

3.5. Influence of quantum tunneling of protons through respiratory complex I on the electrical potential of IMM.

Eventually, the influence of the quantum tunneling of protons through the subunits of complex I on the membrane potential of IMM can be studied. Hence, the effect of the quantum tunneling of protons on the proton motive force (pmf) can be explored. See Figure 10.

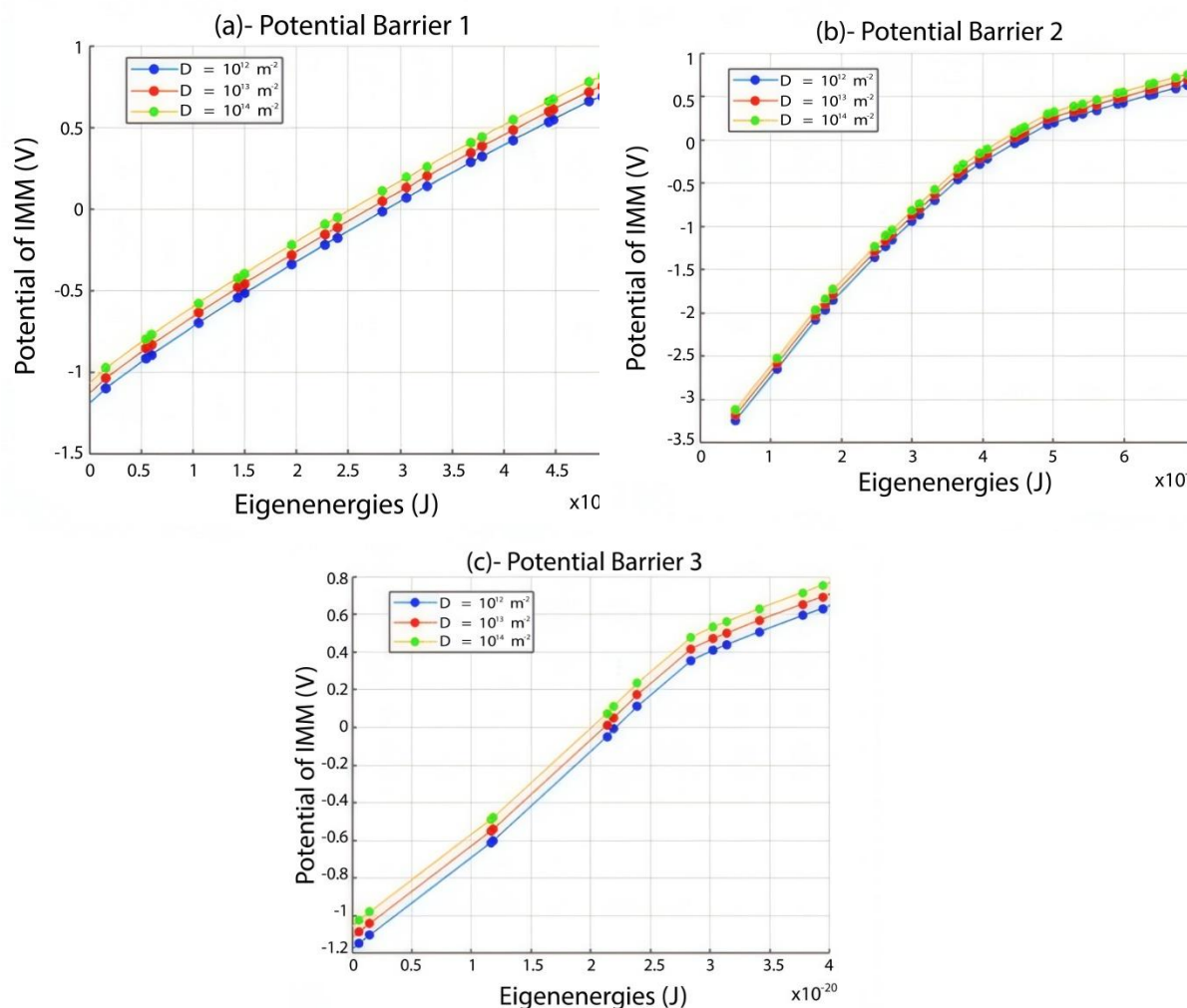


Figure 10. The figure represents the influence of the quantum tunneling of protons on the electrical potential of IMM. The relationship between the electrical potential of IMM and the eigenenergies for (a) barrier 1; (b) barrier 2; (c) barrier 3.

3.6. Discussion.

Quantum biology is an emerging field that aims to investigate the quantum mechanical aspects of biological processes. Mitochondria represent an interesting molecular target to explore the role of the quantum behavior of protons in maintaining the vital function of energy production. In the present work, we investigated the transport of protons via quantum tunneling through a major component of ETC, which is respiratory complex I. Based on the literature, three major potential barriers were identified and used to study the quantum tunneling transport of protons. Eigen-energies were obtained for each barrier by solving the Schrödinger equation, and each barrier showed a different set of them. The quantum tunneling probability of protons through barrier 1 is within the range of 9.9×10^{-30} to near 1, and from 1.23×10^{-64} to near 1 for barrier 2, and from 1.44×10^{-30} to near 1 for barrier 3. These values of tunneling probabilities

correspond to the lowest energy state higher than zero and the highest state near the highest point in the potential function, respectively. See Figure 5.

On the other hand, the probability that a proton can obtain sufficient energy to go through barrier 1 according to the Boltzmann distribution (the classical probability) is estimated by $\exp\left(\frac{-(5+3.5)\times 10^{-20}}{K_B T}\right) = 2.6 \times 10^{-9}$, and the probabilities for barrier 2 and barrier

3 are estimated by $\exp\left(\frac{-(5+6.5+2.4)\times 10^{-20}}{K_B T}\right) = 9.38 \times 10^{-15}$ and

$\exp\left(\frac{-(4.6+0.8)\times 10^{-20}}{K_B T}\right) = 3.43 \times 10^{-6}$, respectively. See Figure 3. By close observation of these

values, it is clear that quantum tunneling is an energy-saving type of transport, while classical transport is less efficient in terms of energy requirements. This is because quantum tunneling transport can yield a tunneling probability of 1.2×10^{-9} through barrier 1 at the eigenenergy of 3.26×10^{-20} J, which means quantum tunneling utilizes only around 38% of the total energy required to overcome barrier 1 classically to achieve the same or near the value of the classical probability. For barrier 2, protons can tunnel with a probability of 1.92×10^{-16} at an eigenenergy of 4.07×10^{-20} J, which means quantum tunneling utilizes only 29% of the total energy required to overcome barrier 2 classically to achieve the same or near the value of the classical probability. For barrier 3, protons can tunnel with a probability of 3.77×10^{-6} at an eigenenergy of 2.84×10^{-20} J, which means quantum tunneling utilizes only 47% of the total energy required to overcome barrier 3 classically to achieve the same or near the value of the classical probability.

In addition, the quantum unitary conductance of protons of barrier 1 ranges from around 3.85×10^{-34} S to around 3.88×10^{-5} S and from 4.75×10^{-69} S to around 3.88×10^{-5} S for barrier 2 and from around 5.57×10^{-35} S to around 3.88×10^{-5} S for barrier 3. See Figure 6. Moreover, the quantum membrane conductance is within the range of $(3.85 \times 10^{-22} - 3.88 \times 10^9)$ S/m² for barrier 1, and within the range of $(4.76 \times 10^{-55} - 3.88 \times 10^9)$ S/m² for barrier 2 and within the range of $(5.57 \times 10^{-23} - 3.88 \times 10^9)$ S/m² for barrier 3, as represented in Figure 7. However, the classical membrane conductance value of the IMM itself is within the magnitude of 10^{-5} S/m² [21] and within the magnitude of 10^{-2} S/m² for ETC complexes [20] to generate the electrical potential of IMM. If these values are compared, quantum tunneling provides a very wide range of quantum conductance values, which absolutely includes the physiological values required for generating the electrical potential of IMM.

The quantum tunneling delay time, which is time spent by the proton in the barrier, is another important physical entity studied in the present work. For barrier 1, the proton has a delay time within an order of magnitude of 10^{-13} s for most of its eigen-energies except for the second energy state, which corresponds to a very long tunneling delay time of 2.1×10^3 s. This is attributed to the complexity of the potential function and the quantum wave behavior inferred from the wave function. However, protons that tunnel through barrier 2 have different patterns of tunneling delay time. They tunnel through barrier 2 with delay time within a wide range of $(10^3 - 10^{-13})$ s for eigenenergies between zero and 5×10^{-20} J, while they tunnel with a tunneling delay time of 10^{-13} s for eigenenergies higher than 5×10^{-20} . Moreover, protons tunnel through barrier 3 with a delay time of 10^{-13} s except for eigenenergies 1.486×10^{-21} J and 2.387×10^{-20} J, which correspond to tunneling delay times 476.6 s and 6.37×10^{-11} s, respectively. See Figure 8. As we said before, these exceptions emerge due to the complexity of the potential and

quantum wave functions. Therefore, most of the quantum states experience a tunneling delay time in the order of magnitude of 10^{-13} s when the proton tunnels through the potential barriers of the respiratory complex I. These values obtained are consistent with the values calculated for proton tunneling in DNA nucleotide base pairs [18,19]. The tunneling delay time of proton transfer between Guanine and Cytosine in DNA double helix is within the magnitude of 10^{-13} s [18], while the tunneling delay time of proton transfer within the Guanine base itself is within the magnitude of 10^{-12} s [19]. In addition, the entropic tunneling time has been applied to the tunneling of potassium ions in telomeric G-quadruplex systems, and it was found to be within the magnitude of 10^{-10} s [25].

Additionally, as a result of quantum tunneling, a tunneling current of protons is expected to be estimated. The values of the tunneling current are within the range of $(1.6 \times 10^{-48} - 5.96 \times 10^{-7})$ A, $(2.27 \times 10^{-85} - 1.38 \times 10^{-6})$ A, and $(2.55 \times 10^{-51} - 1.58 \times 10^{-6})$ A for barrier 1, barrier 2 and barrier 3, respectively. See Figure 9. Again, quantum tunneling offers a very wide range of electrical current values. As we said before, the quantum tunneling transport can occur at proton energy values less than the height of the barrier, and this allows the existence of several values of tunneling probability, tunneling current, and quantum conductance.

Eventually, it is expected that the electrical activity mediated by quantum tunneling can affect the electrical potential of IMM. According to Figure 10, each barrier alone can set the electrical potential of IMM within the physiological range of 150-200 mV. However, only certain values are allowed according to the permitted energies of protons. For barrier 1, the eigenenergies between $(2.5 - 3.5) \times 10^{-20}$ J are capable of generating a membrane potential within the physiological range of normal functioning. For barrier 2 and barrier 3, they are the eigenenergies within the range of $(4.5 - 5) \times 10^{-20}$ J and $(2 - 2.5) \times 10^{-20}$ J, respectively. According to these ranges, quantum tunneling can influence the potential of IMM while minimizing the energy requirements compared to classical transport. Classically, an energy equivalent or higher than the sum of barrier heights is required for classical transport to occur and thus to have an effect on certain biological systems. Based on these observations, quantum tunneling allows mitochondria to use a fraction of the energy required to overcome the barrier compared to classical transport, which uses 100% or even higher to overcome the barrier. For barrier 1, protons with an average eigenenergy of 3×10^{-20} J use 35% of the total energy required to go through the barrier classically to generate a membrane potential within the physiological range, while protons of barrier 2 with an average eigenenergy of 4.75×10^{-20} J and protons of barrier 3 with an average eigenenergy of 2.25×10^{-20} J use 34% and 42% of the total energy to generate a physiological membrane potential, respectively.

Furthermore, even though each barrier has a limited number of allowed values for electrical potential, combining the influence of the three subunits and the contribution of the number of complex I proteins will provide a much wider range of allowed values for electrical potential. This might provide the mitochondria with better control over the available resources of proteins and energy, thus increasing their efficiency in producing and sustaining the sources of energy for cells and their resilience in fighting cellular stress before reaching the apoptotic or necrotic stage. Moreover, each barrier has a buffering property by which quantum tunneling of protons can exceed substantially the classical membrane conductance of 4×10^{-5} S/m², resulting in large hyperpolarization reaching 800 mV, or it can be much lower than the classical conductance, resulting in large depolarization reaching 0 mV or reversed electrical potential of IMM. This allows mitochondria to adjust the membrane potential to keep it within the

physiological range when the classical membrane conductance changes substantially from its baseline value due to cellular pathologies [26–30].

4. Conclusions

Accordingly, quantum tunneling might be a crucial quantum biological process for optimizing and sustaining the functionality of the mitochondrion and supporting its adaptation under cellular stress. This is guaranteed by the lower energy requirement for the tunneling of protons, the more controlled utilization of the number of subunits of complex I and the total number of complex I proteins, and the ability to adapt to the dramatic changes in the mitochondrial membrane permeability and maintain a physiological electrical potential for IMM.

Author Contributions

Conceptualization, A.B.Q., H.R.M., H.L., R.A., A.A., S.K., M.M., R.A., M.A.A., Z.A., Y.A., D.E., R.A., D.D., R.A., N.A., A.H., M.A., A.A.I. A.A., A.A. M.B., J.F.A.; methodology, A.B.Q.; software, A.B.Q.; validation, A.B.Q., H.R.M., H.L., R.A., A.A., S.K., M.M., R.A., M.A.A., Z.A., Y.A., D.E., R.A., D.D., R.A., N.A., A.H., M.A., A.A.I. A.A., A.A. M.B., J.F.A.; formal analysis, A.B.Q. and J.F.A.; investigation, A.B.Q., H.R.M., H.L., R.A., A.A., S.K., M.M., R.A., M.A.A., Z.A., Y.A., D.E., R.A., D.D., R.A., N.A., A.H., M.A., A.A.I. A.A., A.A. M.B., J.F.A.; resources, A.B.Q., H.R.M., H.L., R.A., A.A., S.K., M.M., R.A., M.A.A., Z.A., Y.A., D.E., R.A., D.D., R.A., N.A., A.H., M.A., A.A.I. A.A., A.A. M.B., J.F.A.; data curation, A.B.Q.; writing—original draft preparation, A.B.Q., H.R.M., H.L., R.A., A.A., S.K., M.M., R.A., M.A.A., Z.A., Y.A., D.E., R.A., D.D., R.A., N.A., A.H., M.A., A.A.I. A.A., A.A. M.B., J.F.A.; writing—review and editing, A.B.Q., H.R.M., H.L., R.A., A.A., S.K., M.M., R.A., M.A.A., Z.A., Y.A., D.E., R.A., D.D., R.A., N.A., A.H., M.A., A.A.I. A.A., A.A. M.B., J.F.A.; visualization, A.B.Q.; supervision, A.B.Q. and J.F.A.; project administration, A.B.Q. and J.F.A.

Institutional Review Board Statement

Not applicable.

Informed Consent Statement

Not applicable.

Data Availability Statement

Data supporting the findings of this study are available upon reasonable request from the corresponding author.

Funding

This research received no external funding.

Acknowledgments

None.

Conflicts of Interest

The authors declare no conflict of interest

References

1. Tábara, L.-C.; Segawa, M.; Prudent, J. Molecular mechanisms of mitochondrial dynamics. *Nat. Rev. Mol. Cell Biol.* **2025**, *26*, 123–146, <https://doi.org/10.1038/s41580-024-00785-1>.
2. Suomalainen, A.; Nunnari, J. Mitochondria at the crossroads of health and disease. *Cell* **2024**, *187*, 2601–2627, <https://doi.org/10.1016/j.cell.2024.04.037>.
3. Zotta, A.; O'Neill, L.A.J.; Yin, M. Unlocking potential: the role of the electron transport chain in immunometabolism. *Trends Immunol* **2024**, *45*, 259–273, <https://doi.org/10.1016/j.it.2024.02.002>.
4. Zhang, Y.; Marcillat, O.; Giulivi, C.; Ernster, L.; Davies, K.J. The oxidative inactivation of mitochondrial electron transport chain components and ATPase. *J. Biol. Chem.* **1990**, *265*, 16330–16336, [https://doi.org/10.1016/S0021-9258\(17\)46227-2](https://doi.org/10.1016/S0021-9258(17)46227-2).
5. Röpke, M.; Saura, P.; Riepl, D.; Pöverlein, M.C.; Kaila, V.R.I. Functional Water Wires Catalyze Long-Range Proton Pumping in the Mammalian Respiratory Complex I. *J. Am. Chem. Soc.* **2020**, *142*, 21758–21766, <https://doi.org/10.1021/jacs.0c09209>.
6. Grba, D.N.; Chung, I.; Bridges, H.R.; Agip, A.-N.A.; Hirst, J. Investigation of hydrated channels and proton pathways in a high-resolution cryo-EM structure of mammalian complex I. *Sci Adv* **2023**, *9*, eadi1359, <https://doi.org/10.1126/sciadv.adi1359>.
7. Zdorevskiy, O.; Djurabekova, A.; Lasham, J.; Sharma, V. Horizontal proton transfer across the antiporter-like subunits in mitochondrial respiratory complex I. *Chem. Sci.* **2023**, *14*, 6309–6318, <https://doi.org/10.1039/d3sc01427d>.
8. Madl, P.; Renati, P. Quantum Electrodynamics Coherence and Hormesis: Foundations of Quantum Biology. *Int. J. Mol. Sci.* **2023**, *24*, 14003, <https://doi.org/10.3390/ijms241814003>.
9. Kinsey, L.J.; Beane, W.S.; Tseng, K.A.-S. Accelerating an integrative view of quantum biology. *Front. Physiol.* **2024**, *14*, 1349013, <https://doi.org/10.3389/fphys.2023.1349013>.
10. Pushkaran, A.C.; Arabi, A.A. A review on point mutations *via* proton transfer in DNA base pairs in the absence and presence of electric fields. *Int. J. Biol. Macromol.* **2024**, *277*, 134051, <https://doi.org/10.1016/j.ijbiomac.2024.134051>.
11. Korchagina, K.; Balasubramani, S.G.; Berreur, J.; Gerard, E.F.; Johannissen, L.O.; Green, A.P.; Hay, S.; Schwartz, S.D. Directed Evolution's Selective Use of Quantum Tunneling in Designed Enzymes—A Combined Theoretical and Experimental Study. *J. Phys. Chem. B* **2025**, *129*, 1555–1562, <https://doi.org/10.1021/acs.jpcc.4c08169>.
12. Bennett Jr., J.P.; Onyango, I.G. Energy, Entropy and Quantum Tunneling of Protons and Electrons in Brain Mitochondria: Relation to Mitochondrial Impairment in Aging-Related Human Brain Diseases and Therapeutic Measures. *Biomedicines* **2021**, *9*, 225, <https://doi.org/10.3390/biomedicines9020225>.
13. Moser, C.C.; Farid, T.A.; Chobot, S.E.; Dutton, P.L. Electron tunneling chains of mitochondria. *Biochim. Biophys. Acta - Bioenerg.* **2006**, *1757*, 1096–1109, <https://doi.org/10.1016/j.bbabbio.2006.04.015>.
14. Nunn, A.V.W.; Guy, G.W.; Bell, J.D. The quantum mitochondrion and optimal health. *Biochem. Soc. Trans.* **2016**, *44*, 1101–1110, <https://doi.org/10.1042/BST20160096>.
15. Serway, R.; Jewett, J. Physics for Scientists and Engineers with Modern Physics. 10th Edition; Cengage Learning, Boston, Massachusetts, USA: **2018**.
16. Atom Tunneling Phenomena in Physics, Chemistry and Biology. Miyazaki, T., Ed.; Springer Series on Atomic, Optical, and Plasma Physics; Springer: Berlin, Heidelberg, **2004**; Volume 36, <https://doi.org/10.1007/978-3-662-05900-5>.
17. Hill, B. Ion Channels of Excitable Membranes, 3rd Edition; Sinauer Associates, Inc.:Sunderland, Massachusetts, USA: **2001**.
18. Çelebi, G.; Özçelik, E.; Vardar, E.; Demir, D. Time delay during the proton tunneling in the base pairs of the DNA double helix. *Prog. Biophys. Mol. Biol.* **2021**, *167*, 96–103, <https://doi.org/10.1016/j.pbiomolbio.2021.06.001>.
19. Özçelik, E.; Akar, D.E.; Zaman, S.; Demir, D. Time delay during intra-base proton tunneling in the guanine base of the single stranded DNA. *Prog. Biophys. Mol. Biol.* **2022**, *173*, 4–10, <https://doi.org/10.1016/j.pbiomolbio.2022.05.009>.

20. Abdallat, M.; Qaswal, A.B.; Eftaiha, M.; Qamar, A.R.; Alnajjar, Q.; Sallam, R.; Kollab, L.; Masa'deh, M.; Amayreh, A.; Mihyar, H.; Aboushakra, H.; Alkelani, B.; Owaimer, R.; Abd-Alhadi, M.; Ireiqat, S.; Turk, F.; Daoud, A.; Darawsheh, B.; Hiasat, A.; Alhalaki, M.; Abdallat, S.; Hamad, S.B.; Murshidi, R. A mathematical modeling of the mitochondrial proton leak via quantum tunneling. *AIMS Biophysics* **2024**, *11*, 189–233, <https://doi.org/10.3934/biophy.2024012>.
21. Gutknecht, J. Proton/Hydroxide Conductance and Permeability through Phospholipid Bilayer Membranes. *Proc. Natl. Acad. Sci. U S A* **1987**, *84*, 6443–6446, <https://doi.org/10.1073/pnas.84.18.6443>.
22. Ansari, F.; Yoval, B.; Niatetskaya, Z.; Ten, V.; Wittig, I.; Galkin, A. How many molecules of mitochondrial complex I are in a cell?. *nal. Biochem.* **2022**, *646*, 114646, <https://doi.org/10.1016/j.ab.2022.114646>.
23. Cole, L.W. The Evolution of Per-Cell Organelle Number. *Front. Cell Dev. Biol.* **2016**, *4*, 85, <https://doi.org/10.3389/fcell.2016.00085>.
24. Mannella, C.A.; Lederer, W.J.; Jafri, M.S. The connection between inner membrane topology and mitochondrial function. *J. Mol. Cell. Cardiol.* **2013**, *62*, 51–57, <https://doi.org/10.1016/j.yjmcc.2013.05.001>.
25. Celebi Torabfam, G.; Demir, G.K.; Demir, D. Quantum tunneling time delay investigation of K^+ ion in human telomeric G-quadruplex systems. *J. Biol. Inorg. Chem.* **2023**, *28*, 213–224, <https://doi.org/10.1007/s00775-022-01982-z>.
26. Carroll, J.; He, J.; Ding, S.; Fearnley, I.M.; Walker, J.E. Persistence of the permeability transition pore in human mitochondria devoid of an assembled ATP synthase. *Proc. Natl. Acad. Sci. U S A* **2019**, *116*, 12816–12821, <https://doi.org/10.1073/pnas.1904005116>.
27. Su, L.; Xu, J.; Lu, C.; Gao, K.; Hu, Y.; Xue, C.; Yan, X. Nano-flow cytometry unveils mitochondrial permeability transition process and multi-pathway cell death induction for cancer therapy. *Cell Death Discov.* **2024**, *10*, 176, <https://doi.org/10.1038/s41420-024-01947-y>.
28. Baev, A.Y.; Vinokurov, A.Y.; Potapova, E.V.; Dunaev, A.V.; Angelova, P.R.; Abramov, A.Y. Mitochondrial Permeability Transition, Cell Death and Neurodegeneration. *Cells* **2024**, *13*, 648, <https://doi.org/10.3390/cells13070648>.
29. Vringer, E.; Tait, S.W.G. Mitochondria and cell death-associated inflammation. *Cell Death Differ.* **2023**, *30*, 304–312, <https://doi.org/10.1038/s41418-022-01094-w>.
30. Vandenabeele, P.; Bultynck, G.; Savvides, S.N. Pore-forming proteins as drivers of membrane permeabilization in cell death pathways. *Nat. Rev. Mol. Cell Biol.* **2023**, *24*, 312–333, <https://doi.org/10.1038/s41580-022-00564-w>.

Publisher's Note & Disclaimer

The statements, opinions, and data presented in this publication are solely those of the individual author(s) and contributor(s) and do not necessarily reflect the views of the publisher and/or the editor(s). The publisher and/or the editor(s) disclaim any responsibility for the accuracy, completeness, or reliability of the content. Neither the publisher nor the editor(s) assume any legal liability for any errors, omissions, or consequences arising from the use of the information presented in this publication. Furthermore, the publisher and/or the editor(s) disclaim any liability for any injury, damage, or loss to persons or property that may result from the use of any ideas, methods, instructions, or products mentioned in the content. Readers are encouraged to independently verify any information before relying on it, and the publisher assumes no responsibility for any consequences arising from the use of materials contained in this publication